Synthesis, Structure, and Magnetic Characterization of Pulsed Laser-Ablated Superconducting $La_2CuO_4F_x$ Thin Films

S. T. Lees, I. Gameson, M. O. Jones, and P. P. Edwards*

School of Chemistry, The University of Birmingham, Edgbaston, Birmingham B15 2TT, U.K.

M. Slaski

School of Physics and Astronomy, The University of Birmingham, Edgbaston, Birmingham B15 2TT, U.K.

Received April 13, 1998. Revised Manuscript Received July 2, 1998

High quality, *c*-axis oriented thin films of semiconducting La_2CuO_4 have been fabricated by pulsed laser-ablation deposition. Superconducting properties have been successfully induced in the films by a postdeposition, ex-situ static annealing process in a F_2/N_2 gas mixture. The influence of the fluorination temperature on the structural, magnetic, and electronic properties of the resulting thin films has been examined in detail. X-ray data reveal that facile fluorination of the films proceeds via a complex, multistage process, often yielding two distinct La_2CuO_4-type phases. This phase segregation suggests a disproportionation process following fluorine uptake. Such a disproportionation is subtly different from that found for oxygen excess La_2CuO_4 in that for $La_2CuO_{4+\delta}$ the parent O_4 and an oxygen rich ($O_{4+\delta}$) phase are formed, but in the present system two fluorinated (i.e., oxidized) phases are formed. La_2CuO_4 thin films fluorinated at a temperature of 150 °C possess the highest values for both T_c (onset) (ca. 38.5 K) and critical current density ($>10^6$ A cm^{-2} at 4.2 K in zero magnetic field). Magnetic susceptibility data demonstrate that this fluorination methodology is of sufficient sensitivity to allow the controlled hole-doping of semiconducting La_2CuO_4 thin films through to the high-temperature superconducting regime.

Introduction

Pulsed laser-ablation has now emerged as a powerful and versatile thin film deposition technique that enjoys particular success in the fabrication of high transition temperature (T_c) superconducting films,[1,2] among other advanced electronic materials. Within the field of high T_c superconducting films, the majority of reports have focused on the fabrication of thin film phases that superconduct either as-deposited or upon (oxidative) treatment within the laser-ablation chamber itself. Relatively little attention has been afforded to the development of postdeposition, ex-situ treatments on nonsuperconducting "precursor" films; such an approach takes on particular importance when one wishes to introduce highly reactive or potentially toxic species without the attendant contamination and damage to the ablation chamber and apparatus. Pioneering work on the electrochemical oxygen intercalation of *c*-axis $La_2CuO_{4+\delta}$ thin films was carried out by Locquet and coworkers.[3,4] These authors demonstrated that electrochemical oxidation occurs via a two step mechanism. First, oxygen is transported into the film by intercalation into planar defects which arise from the lattice mismatch between the thin film and the substrate. This initial step is followed by a second, slower step in which oxygen diffusion into the interstial sites occurs via the *ab* planes. Recently, we have developed a postdeposition, ex-situ fluorination methodology that can be used to controllably oxidize (i.e., hole dope) thin film cuprate materials. To illustrate the potential of this approach, we report here the results of its application to the La_2CuO_4 system.

Stoichiometric La_2CuO_4 (Figure 1a) is an antiferromagnetic semiconductor, but this localized electronic behavior transforms continuously to delocalized character when the electronically active CuO_2 sheets are partially oxidized and excess holes are introduced into the valence band. This oxidation (i.e., hole doping) therefore effects a semiconductor-to-metal transition in the material at temperatures above T_c. On cooling, hole-doped La_2CuO_4 exhibits high temperature superconductivity over a relatively narrow composition range coincident with this transition. This electronic behavior is shown schematically in Figure 2.[5] One notes that

* Corresponding author. Telephone: 44 121 414 3530. Fax: 44 121 414 4442. E-mail: p.p.edwards@bham.ac.uk.

(1) *Laser-Ablation in Materials Processing: Fundamentals and Applications*; Brareu, B., Fubowski, J. J., Norton, D. P., Eds.; MRS Symp. Proc. *285*, 1993.

(2) Christy, D. R.; Huber, G. *Pulsed Laser Deposition of Thin Films*; John Wiley & Sons: New York, 1994.

(3) Locquet, J.-P.; Gerber, C.; Cretton, A.; Jaccard, Y.; Williams E. J.; Machler, E. *Appl. Phys. A* **1993**, *57*, 211.

(4) Arrouy, F.; Locquet, J.-P.; Williams, E. J.; Machler, E.; Berger, R.; Gerber, C.; Monroux, C.; Grenier, J.-C.; Wattiaux, A. *Phys. Rev. B* **1996**, *54*, 7512.

(5) Prassides, K.; Lappas, A. *Chem. Br.* **1994**, *30*, 730.

10.1021/cm9802752 CCC: $15.00
Published on Web 09/24/1998

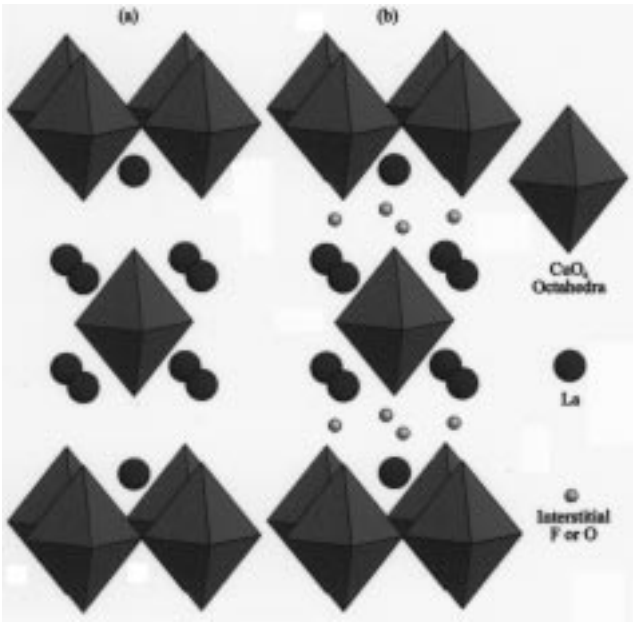

Figure 1. Crystal structures of (a) La_2CuO_4 and (b) $La_2CuO_4F_x$ (for simplicity the slight orthorhombic distortion is not shown).

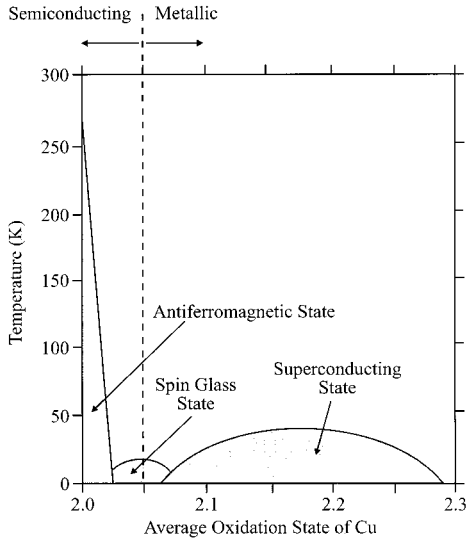

Figure 2. Schematic representation of the evolution of electronic behavior as positive holes are introduced into the valence band of La_2CuO_4.

there is an optimum concentration of holes in the valence band, corresponding to an average Cu oxidation state of ca. +2.17, at which the superconducting transition temperature of the superconductor is maximized. At this point, the material is said to be optimally doped.

Manipulation of the carrier concentration to induce superconductivity in La_2CuO_4 has routinely been accomplished by either partial aliovalent substitution of La^{3+} with alkali or alkaline-earth cations[6−11] or the insertion of interstitial anions such as oxide[12−20] or fluoride[21−23] into the crystal lattice. Tissue et al.[21] first reported the conversion of bulk, polycrystalline La_2CuO_4 into a high-temperature superconductor by an oxidative treatment in F_2 gas. It has since been shown that under optimized conditions (1.3 bar of pure F_2 gas, 200 °C, 20 h) fluorination of bulk prepared La_2CuO_4 yields a virtually monophasic product with a T_c of 40 K.[22,23] The fluorination causes a significant enhancement of the *c*-lattice parameter and neutron diffraction and EXAFS measurements at the La L_{III} X-ray absorption edge indicate that the fluorinated structure contains additional anions between consecutive LaO layers as indicated in Figure 1b.[24,25]

In a recent, preliminary communication we have reported that superconducting properties can be induced in pulsed laser-ablated, semiconducting thin films of La_2CuO_4 by a postdeposition, ex-situ gas-phase fluorination approach.[26] In the present work we report the development and optimization of this fluorination methodology. In particular, we focus on the influence of the fluorination temperature, T_{F_2}, on the structural, magnetic, and electronic properties of the resulting films. The evolution of structural and electronic properties within the films is examined in some detail and comparisons are made with bulk prepared samples.

We believe that the development of postdeposition ex-situ treatments on precursor films will become increasingly important in the evolving materials chemistry of thin films. The present strategy of the controlled, ex-situ hole-doping of electronic thin film materials may also have wide applicability, not only being extended to different families of high T_c and other materials but

(6) Bednorz, J. G.; Müller, K. A. *Z. Phys. B* **1986**, *64*, 189.
(7) Tarascon, J. M.; Greene, L. H.; McKinnon, W. R.; Hull, G. W.; Geballe, T. H. *Science* **1987**, *235*, 1373.
(8) Torrance, J. B.; Bezinge, A.; Nazzal, A. I.; Huang, T. C.; Parkin, S. S. P.; Keane, D. T.; LaPlaca, S. J.; Horn, P. M.; Held, G. A. *Phys. Rev. B* **1989**, *40*, 8872.
(9) Axe, J. D.; Moudden, A. H.; Hohlwein, D.; Cox, D. E.; Mohanty, K. M.; Moodenbaugh, A. R.; Xu, Y. *Phys. Rev. Lett.* **1989**, *62*, 2751.
(10) Subramanian, M. A.; Gopalakrishnan, J.; Torardi, C. C.; Askew, T. R.; Flippen, R. B.; Sleight, A. W.; Lin, J. J.; Poon, S. J. *Science* **1988**, *240*, 495.
(11) Torardi, C. C.; Subramanian, M. A.; Gopalakrishnan, J.; Sleight, A. W. *Physica C* **1989**, *158*, 465.
(12) Beille, J.; Chevalier, B.; Demazeau, G.; Deslandes, F.; Etourneau, J.; Laborde, O.; Michel, C.; Lejay, P.; Provost, J.; Raveau, B.; Sulpice, A.; Tholence, J. L.; Tournier, R. *Physica B* **1987**, *146*, 307.
(13) Demazeau, G.; Tresse, F.; Plante, T.; Chevalier, B.; Etourneau, J.; Michel, C.; Hervieu, M.; Raveau, B.; Lejay, P.; Sulpice, A.; Tournier, R. *Physica C* **1988**, *153−155*, 824.
(14) Schirber, J. E.; Morosin, B.; Merrill, M.; Hlava, F.; Venturini, E. L.; Kwak, J. F.; Nigrey, P. J.; Baughman, R. J.; Ginley, D. S. *Physica C* **1988**, *152*, 121.
(15) Wattiaux, A.; Park, J. C.; Grenier, J. C.; Pouchard, M. *C. R. Acad. Sci. Paris* **1990**, *310*, 1047.
(16) Grenier, J. C.; Wattiaux, A.; Lagueyte, N.; Park, J. C.; Marquestaut, E.; Etourneau, J.; Pouchard, M. *Physica C* **1991**, *173*, 139.
(17) Grenier, J. C.; Lagueyte, N.; Wattiaux, A.; Doumerc, J. P.; Dordor, P.; Etourneau, J.; Pouchard, M.; Goodenough, J. B.; Zhou, J. S. *Physica C* **1992**, *202*, 209.
(18) Rudolf, P.; Schöllhorn, R. *J. Chem. Soc., Chem. Commun.* **1992**, 1158.
(19) Takayama-Muromachi, E.; Sasaki, T.; Matsui, Y. *Physica C* **1993**, *207*, 97.
(20) Takayama-Muromachi, E.; Navrotsky, A. *Physica C* **1993**, *218*, 164.
(21) Tissue, B. M.; Cirillo, K. M.; Wright, J. C.; Daeumling, M.; Larbalestier, D. C. *Solid State Commun.* **1988**, *65*, 51.
(22) Chevalier, B.; Tressaud, A.; Lepine, B.; Amine, K.; Dance, J. M.; Lozano, L.; Hickey, E.; Etourneau, J. *Physica C* **1990**, *167*, 97.
(23) Chevalier, B.; Tressaud, A.; Lepine, B.; Robin, C.; Etourneau, J. *J. Less-Common Met.* **1990**, *164−165*, 832.
(24) Chevalier, B.; Tressaud, A.; Robin, C.; Lepine, B.; Tuilier, M. H.; Soubeyroux, J. L.; Etourneau, J. *ICMAS 91*; Raveau, B., Wasa, K., Suryanaryanan, R., Eds.; IITT Paris 21, 1991.
(25) Tuilier, M. H.; Chevalier, B.; Tressaud, A.; Brisson, C.; Soubeyroux, J. L.; Etourneau, J. *Physica C* **1992**, *200*, 113.
(26) Lees, S. T.; Gameson, I.; Jones, M. O.; Edwards, P. P.; Greaves, C.; Wellhofer, F.; Woodall, P.; Langford, I.; Slaski, M. *Physica C* **1996**, *270*, 305.

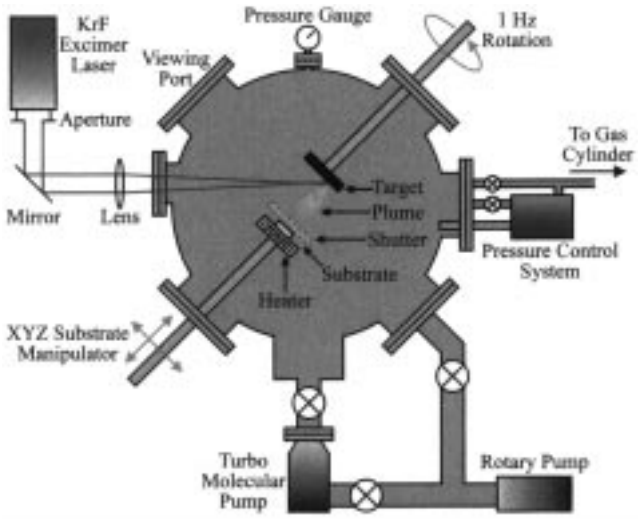

Figure 3. Schematic representation of the laser-ablation apparatus.

Table 1. Pulsed Laser-Ablation Deposition Conditions for La_2CuO_4 Thin Films

laser	KrF excimer
laser wavelength	248 nm
laser pulse length	20 ns
laser repetition rate	10 Hz
laser pulse fluence	ca. 1.5 J cm^{-2}
laser spot size on target	5 mm × 2 mm
substrate	5 mm × 5 mm (100) $SrTiO_3$
substrate temp	760 °C
target−substrate distance	7 cm
deposition gas	high purity O_2
deposition gas pressure	400 mTorr
deposition time	15 min

also as a potential method for patterning superconducting thin films.[27]

Experimental Section

Target pellets of polycrystalline La_2CuO_4 were prepared by standard solid state techniques. Accurately weighed, stoichiometric quantities of dry, high purity La_2O_3 and CuO powders were intimately mixed, pelletized, and fired in air at 1050 °C for 24 h. Powder X-ray diffraction data, collected on a Siemens D-5000 diffractometer (Cu Kα1), were used to confirm that monophasic La_2CuO_4 had formed.

Thin films of La_2CuO_4 were fabricated by pulsed laser-ablation from the oxide target pellets by using the optimal deposition conditions that were determined in our previous work[26] (and which are summarized in Table 1). A schematic representation of the laser-ablation apparatus is shown in Figure 3. In this method, a slowly rotating pellet of the target material is irradiated by a KrF UV laser. This produces a plasmatic plume with the same stoichiometry as the target. The plume migrates across the ablation chamber and deposits as a thin film on a heated substrate crystal. (The substrate material is carefully selected so as to minimize the lattice mismatch between it and the thin film phase.) After following the ablation conditions summarized in Table 1, O_2 gas was introduced into the chamber to a pressure of 1 atm while the film temperature was maintained at 760 °C in order to ensure that stoichiometric oxygen uptake had occurred within each of the films. The films were then allowed to cool to room temperature before being removed from the ablation chamber. All films prepared by this process were found to be semiconducting.

(27) Lees, S. T.; Gameson, I.; Jones, M. O.; Edwards, P. P., Bari, M.; Severac, C., in preparation.

Fluorine doping of the resulting La_2CuO_4 films was achieved via a gaseous fluorination approach with an apparatus specifically designed for handling F_2 gas. Given the hazardous nature of F_2 gas, we have included a brief description of the apparatus used, and a schematic diagram of the fluorination equipment is shown in Figure 4. The sample to be fluorinated is placed inside a furnace which is connected to two gas inlet lines and one gas outlet line. The first of the gas inlet lines is connected to the fluorine source (in this case a 10% F_2/90% N_2 gas mixture) while the second inlet line carries dry N_2 which is used to flush out the system. It is essential that no moisture enters the apparatus as the resulting HF would cause significant damage. Thus the N_2 flushing gas is dried by passing it through a bubbler of concentrated sulfuric acid and a silica gel/molecular sieve column. In addition, any traces of HF in the fluorine source supply is removed by a NaF column. The outlet line is connected to a column packed with NaOH pellets. These react with any F_2 that passes through the furnace, thus preventing the release of F_2 gas from the apparatus.

The initial experiments on fluorinating the La_2CuO_4 films were carried out under an atmosphere of flowing 10% F_2/90% N_2 in the temperature range $100 \leq T_{F_2} \leq 200$ °C. However, even under these relatively mild fluorination conditions the hot, flowing gas effectively stripped the surface from the cuprate films. To eliminate this surface damage it was essential to anneal the films under a static gas atmosphere. The films were therefore inserted into the fluorination furnace at room temperature and this was subsequently filled with an atmosphere of 10% F_2/90% N_2. Heating cycles were then programmed into the temperature controller and the La_2CuO_4 films were annealed in these static F_2/N_2 atmospheres in the temperature range $40 \leq T_{F_2} \leq 300$ °C over 10-min periods. After the annealing process, to further minimize the risk of surface damage to the films, the furnace temperature was allowed to cool to room temperature before the F_2/N_2 gas mixture was flushed from the interior with dried N_2 gas. When all traces of F_2 were expelled from the furnace the films were removed and investigated by a variety of techniques.

The structural properties of the films, both before and after fluorination, were investigated by using a high-resolution Siemens X-ray diffractometer equipped with an incident beam focusing monochromator (Cu Kα1) operating in the reflection mode. Rutherford backscattering spectrometry (RBS) was performed on a parent La_2CuO_4 thin film to ascertain its thickness. These measurements were carried out at the Radiation Centre of the University of Birmingham using the 3 MV Dynamitron accelerator. Scanning electron microscopy (SEM) was carried out on a JEOL 6300 instrument to examine the surface morphology of the thin films. Magnetic susceptibility measurements were recorded on both a S100 SQUID (superconducting quantum interference device) magnetometer and a 12-T Oxford Instruments VSM (vibrating sample magnetometry).

Results and Discussion

Structural Properties. Indexed X-ray diffraction patterns from a bulk, polycrystalline La_2CuO_4 target pellet and a La_2CuO_4 thin film deposited from the same pellet are shown in Figure 5. The bulk sample possesses crystallites in every possible orientation and so each symmetry-allowed (*hkl*) reflection for La_2CuO_4 is represented in the observed pattern. The pattern generated from the thin film, however, contains only the (00*l*) reflections and this illustrates conclusively that the film consists of entirely *c*-axis oriented grains. The gaps in the thin film trace at $2\theta = 22.7°$ and 46.5° correspond to the positions of the (100) and (200) reflections of the single-crystal $SrTiO_3$ substrate and data were not collected in these angular regions in order to protect the X-ray detector from their massive intensities. Performing least squares refinements on these data yields

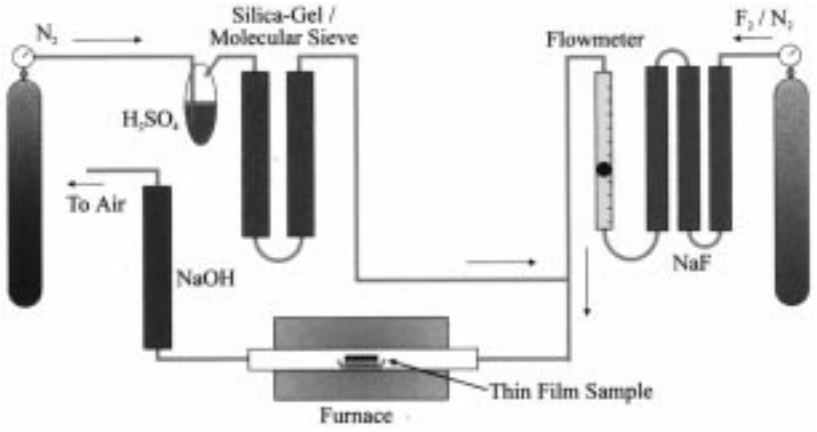

Figure 4. Schematic representation of the fluorination apparatus.

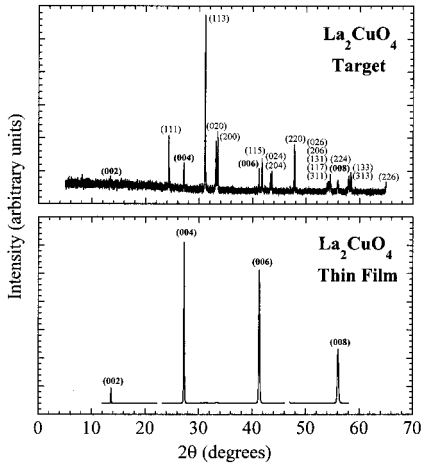

Figure 5. Indexed X-ray diffraction patterns for a bulk, polycrystalline La_2CuO_4 target pellet and a La_2CuO_4 thin film.

values for the *c*-lattice parameters of 13.149(4) and 13.141(2) Å for the bulk and thin film samples, respectively. These are in excellent agreement with the literature value of 13.149(5) Å, obtained from a polycrystalline, bulk prepared sample.[28]

Examination of the X-ray data reveals that all of the films fluorinated with $T_{F_2} < 200$ °C have retained their *c*-axis orientation and there is no evidence of any impurity phase formation. Before conducting a more detailed examination of the influence of T_{F_2} on the structural properties of the fluorinated La_2CuO_4 thin films, the films fluorinated at $T_{F_2} = 70$ and 150 °C will be used to highlight some important structural features. Figure 6 shows a stacked plot of the X-ray diffraction patterns recorded on a parent La_2CuO_4 thin film and on the La_2CuO_4 films fluorinated at 70 and 150 °C. Each of the (00*l*) lines is presented on an expanded 2θ axis so that their peak shapes can be clearly observed. Comparing the X-ray traces from the two fluorinated films with that from the parent film shows that fluorination causes each of the (00*l*) lines to split into two discrete reflections and this implies that there has been some disproportionation following F_2 uptake within the films. Pseudo-Voigt functions have been fitted to these overlapping peaks to reveal their true 2θ positions and this has enabled calculation of the *c*-lattice parameter

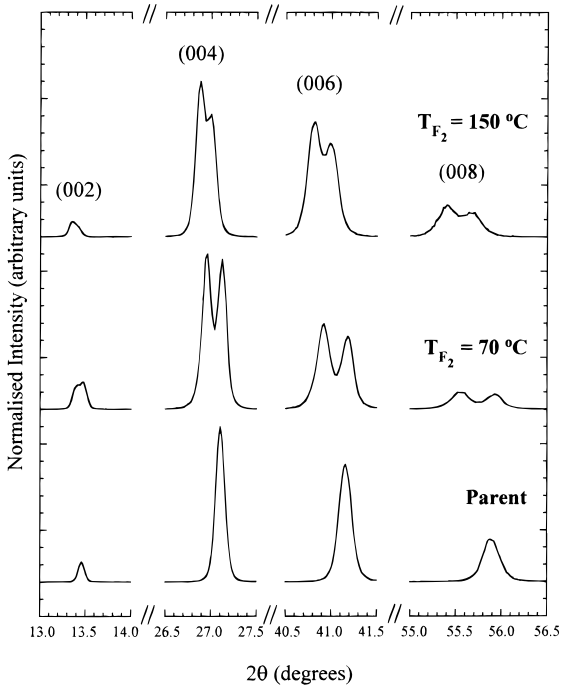

Figure 6. Expanded, normalized, and zero point error corrected (00*l*) X-ray diffraction peaks for a parent La_2CuO_4 thin film and for La_2CuO_4 films fluorinated at $T_{F_2} = 70$ and 150 °C.

of each phase via least squares refinements. In addition, the curve fitting has shown that the relative intensities of the two peaks constituting these doublets are constant for all of the (00*l*) reflections within each of the fluorinated film traces, suggesting that they originate from two La_2CuO_4-type phases having slightly different *c*-lattice parameters.

The results of the *c*-lattice constant refinements on the data from the $T_{F_2} = 70$ °C film give values of 13.144(1) and 13.226(1) Å, suggesting that the film consists of a mixture of the parent and a *c*-axis expanded phase. Indeed, Figure 6 shows that only one of the peaks comprising each doublet has shifted to a lower 2θ value (i.e., a larger *c*-lattice constant) with respect to the peaks from the parent film. The presence of an expanded *c*-lattice phase mirrors the results reported elsewhere on bulk prepared samples and supports the notion that fluorine is incorporated into interstitial sites within the La_2CuO_4 structure causing an increase in the *c*-lattice parameter.[22,23] Least squares refinements on the data

(28) Moorthy, A.; Schmierer, J.; McCarthy, G. *JCPDS [38-709] Grant-in-Aid Report* **1987**.

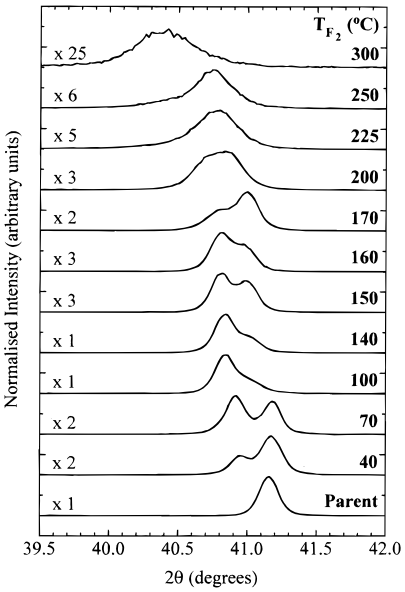

Figure 7. Expanded, normalized, and zero point error corrected (006) X-ray diffraction peaks for parent and fluorinated La_2CuO_4 thin films as a function of fluorination temperature (the normalization factors for each trace are quoted on the left side of the graph).

from the $T_{F_2} = 150$ °C film yield *c*-lattice parameters of 13.196(4) and 13.256(1) Å for the two constituent phases; values which are both significantly larger than the parent La_2CuO_4 phase (c = 13.141(2) Å). This suggests that all of the film is fluorinated (i.e., there is no parent phase remaining) by fluorination at 150 °C and that there is a segregation or disproportionation of the fluorine into two distinct compositions.

These results indicate that there is a continuous evolution of structural properties within the fluorinated films as T_{F_2} is varied. To highlight this effect we show in Figure 7 a normalized stacked plot of the expanded (006) reflections of La_2CuO_4 thin films fluorinated in the range 40 °C $\leq T_{F_2} \leq$ 300 °C along with the parent (006) line. The line shape of each peak is representative of all (00*l*) lines for the film in question. As was observed with the films fluorinated at $T_{F_2} = 70$ and 150 °C, many of the fluorinated films possess (00*l*) lines that are split into two discrete reflections. These X-ray data have been treated in exactly the same way as those from the $T_{F_2} = 70$ and 150 °C films to extract the *c*-lattice parameter of the constituent phases, and the results are presented in Table 2 along with the T_{F_2} administered to each film. The *c*-lattice parameters of the bulk target and parent La_2CuO_4 film are also included for comparative purposes. The data presented in Figure 7 and Table 2 indicate that the variation in structural properties with T_{F_2} are best described in terms of three separate fluorination stages.

First, for $T_{F_2} < 100$ °C, the X-ray data reveal that the fluorinated films consist of a mixture of the parent phase and a *c*-axis expanded phase. As T_{F_2} is increased from room temperature to 100 °C, Figure 6 shows that the proportion of *c*-lattice parameter expanded phase within each film increases relative to the parent phase and the film fluorinated at 100 °C has no parent phase remaining. The *c*-lattice parameter of the expanded phase also increases with T_{F_2} (see Table 2), changing from 13.218(1) to 13.238(1) Å as T_{F_2} changes from 40 to 100 °C. This is consistent with an increase in fluorine uptake as T_{F_2} is increased.

Table 2. Refined *c*-Lattice Parameters for Polycrystalline Bulk Target, Parent, and Fluorinated La_2CuO_4 Thin Films

La_2CuO_4 material	T_{F_2}, °C	refined *c*-lattice parameter(s), Å
bulk target		13.149(4)
parent film		13.141(2)
fluorinated film	40	13.144(1), 13.218(1)
fluorinated film	70	13.144(1), 13.226(1)
fluorinated film	100	13.204(7), 13.238(1)
fluorinated film	140	13.194(3), 13.246(1)
fluorinated film	150	13.196(4), 13.256(1)
fluorinated film	160	13.206(2), 13.260(1)
fluorinated film	170	13.197(1), 13.258(3)
fluorinated film	200	13.257(2)
fluorinated film	225	13.266(2)
fluorinated film	250	13.273(2)
fluorinated film	300	13.390(4)

The second fluorination stage occurs for 100 °C $\leq T_{F_2} <$ 200 °C and the X-ray data (see Table 2) show that all films treated in this range consist of two slightly different *c*-axis expanded phases relative to the parent film. The smaller of these two phases has a relatively constant *c*-lattice parameter of ca. 13.20 Å, while the larger phase exhibits an increase in *c* from 13.238(1) to 13.256(1) Å as T_{F_2} increases from 100 to 150 °C. Further increase in T_{F_2} from 150 to 170 °C causes little change in the *c*-lattice parameter of this larger phase; it maintains a value of ca. 13.26 Å. The data in Figure 7 also show that there is a qualitative change in the relative proportions of the two phases as T_{F_2} is altered. At lower fluorination temperatures (ca. 100−140 °C) the phase with the higher *c*-lattice parameter predominates. As T_{F_2} increases, the ratio of the two phases is reduced until at $T_{F_2} = 170$ °C there is a switch and the predominant phase becomes that with the lower *c*-lattice parameter. Possible explanations for this structural behavior will be discussed shortly, in conjunction with comparisons to results on bulk prepared samples.

For La_2CuO_4 thin films fluorinated with $T_{F_2} \geq 200$ °C, the line shapes of the (00*l*) lines cannot be resolved into two discrete reflections. The peaks from these films are significantly broader than those of the parent film and are indicative of a reduction in crystallinity, almost certainly caused by fluorination at such relatively high temperatures. The *c*-lattice parameters show a steady increase from 13.257(2) to 13.273(2) Å as T_{F_2} is increased from 200 to 250 °C. The X-ray data recorded on the $T_{F_2} = 300$ °C thin film indicate a large reduction in crystallinity. Furthermore, as well as the broad (00*l*) lines for the La_2CuO_4 film, the X-ray diffraction pattern shows that the film has partially decomposed into LaF_3 and CuF_2.

These structural results on thin films show significant differences to earlier findings on bulk prepared samples of fluorinated La_2CuO_4. Chevalier et al.[23] reported that treatment of La_2CuO_4 powders under 1.3 bar pressure of pure F_2 for 20 h at 20 °C $\leq T_{F_2} \leq$ 150 °C caused no noticeable change in the X-ray diffraction data of the material. This highlights the sensitivity and high reactivity of our thin film materials, which undergo a significant structural change when annealed under a static atmosphere of 10% F_2 in N_2 at a temperature of just 40 °C for 10 min (see Figure 7).

When Chevalier et al.[23] increased the fluorination temperature to 150 °C ≤ T_{F_2} ≤ 230 °C, reaction with the F_2 gas took place and a single phase bulk material was produced. In contrast with the results on our thin films, reaction of the bulk material with the F_2 gas does not produce an intermediate region in which a mixture of the parent phase and a *c*-axis expanded phase coexist within the same sample (see Figure 7). Indeed, the *c*-lattice parameter of this bulk phase smoothly increases from 13.16 to 13.21 Å as T_{F_2} increases from 150 to 230 °C. Bhat et al.[29] also reported production of a single phase material following their low-temperature fluorination (160 °C ≤ T_{F_2} ≤ 250 °C) of bulk $La_2CuO_{4+\delta}$ and again observed a similar increase in the *c*-lattice parameter of the material as the fluorination temperature was raised.

These findings differ markedly from our results on thin film samples. Employment of fluorination temperatures in the range 100 °C ≤ T_{F_2} < 200 °C produce films that have no parent phase remaining (and so the films are completely fluorinated) but these films still consist of two slightly different *c*-axis expanded phases. The *c*-lattice parameter of the smaller of these two phases appears to be independent of T_{F_2}, while the *c*-lattice parameter of the larger of the two phases, which does exhibit a dependence on T_{F_2} below 150 °C, is significantly larger (ca. 0.05 Å) than that observed by Chevalier et al.[23] These authors also reported the formation of an additional phase on moving to higher fluorination temperatures (T_{F_2} > 230 °C). This new phase possesses the tetragonal K_2NiF_4 structure and was indexed with c = 13.07 Å, a value significantly lower than the parent La_2CuO_4 *c*-lattice parameter. It therefore appears that our thin film fluorinations in the range 100 °C ≤ T_{F_2} < 200 °C are producing very different results from those observed with bulk samples, with our two fluorinated compositions having *c*-lattice parameters larger than that of the parent La_2CuO_4.

It is important to note that phase separation is now recognized for both bulk and single-crystal samples of oxygen-rich La_2CuO_4.[30−36] These oxygen-rich materials have been observed to possess a phase diagram with a miscibility gap within which samples segregate into an oxygen-rich La_2CuO_4 phase and the parent stoichiometric La_2CuO_4 phase. Locquet et al.[35] also reported that, on a microscopic scale, the introduction of excess oxygen into La_2CuO_4 (via an electrochemical route) creates metallic and/or superconducting regions in the insulating La_2CuO_4 matrix. Our proposal is that a similar phase segregation is occurring within our thin film samples fluorinated at T_{F_2} < 100 °C (see Figure 7 and Table 2). A related finding is that oxygen-rich bulk samples of La_2CuO_4 with additional oxygen contents that place them beyond the phase separated region of the phase diagram, as described above, can undergo an alternative phase separation when exposed to mild thermal treatments.[37] These treatments have been observed to yield a phase of notable stability (with a *c*-lattice parameter of ca. 13.20 Å) and a phase with a larger oxygen content and hence a larger *c*-lattice parameter. A similar segregation into two oxygen-rich La_2CuO_4 phases has also been observed in chemically oxidized thin films of La_2CuO_4 and, again, one of the phases (with a *c*-lattice parameter of 13.197(2) Å) is of notable stability.[38] It has been postulated that the remarkable stability of these oxygen-rich phases could be due to a one-dimensional ordering of the interstitial oxygen along the *c*-axis, similar to that observed by Xiong et al.[39] with $La_2CuO_{4.045}$ and $La_2CuO_{4.055}$ and Tranquada et al.[40] with $La_2NiO_{4+\alpha}$ (where 0.05 < α < 0.11), giving rise to a *c*-axis staged superstructure. Again, these results could be correlated with our findings on La_2CuO_4 films fluorinated in the range 100 °C ≤ T_{F_2} < 200 °C, in which there appears to be segregation into a stable phase with a *c* parameter of ca. 13.20 Å and a phase that possesses a larger *c*-lattice parameter (see Table 2).

The La_2CuO_4 thin films that were fluorinated with T_{F_2} ≥ 200 °C are clearly losing crystallinity but still exhibit an increase in the *c*-lattice parameter as T_{F_2} is raised, implying that facile uptake of fluorine continues to occur within the films. The values of these *c*-lattice parameters (13.257(2)−13.273(2) Å) are significantly larger than any values reported on fluorinated bulk samples of La_2CuO_4 (ca. 13.21 Å).[23] Indeed, employment of high fluorination temperatures (>230 °C) on bulk samples of La_2CuO_4 initially causes partial decomposition into a new K_2NiF_4-type phase, as described above, and as T_{F_2} is raised further, the bulk samples totally decompose into LaF_3 and CuF_2.[23] The K_2NiF_4-type phase is not observed in the X-ray data recorded on our fluorinated thin film samples of La_2CuO_4, but reflections corresponding to LaF_3 and CuF_2 do appear in the trace recorded on the T_{F_2} = 300 °C thin film.

The RBS data from a parent film confirmed a La:Cu ratio of 2:1 and yielded a value of 3700 (±100) Å for the thickness of the film.

Microscopy. The surface of the La_2CuO_4 films were examined by using scanning electron microscopy (SEM) to assess the morphology and any surface damage caused by the fluorination. In Figure 8 we present SEM images of the parent La_2CuO_4 film, the T_{F_2} = 150 °C film, and the T_{F_2} = 300 °C film under magnifications of ×55 and ×2500. In secondary electron-imaging SEM, rough samples give rise to relief contrast effects, in which elevated parts of the sample appear distinctly lighter in the micrograph.

(29) Bhat, V.; Rao, C. N. R.; Honig, J. M. *Solid State Commun.* **1992**, *81*, 75.
(30) Radaelli, P. G.; Jorgensen, J. D.; R. Kleb, Hunter, B. A.; Chou, F. C.; Johnston, D. C. *Phys. Rev. B* **1994**, *49*, 6239.
(31) Radaelli, P. G.; Jorgensen, J. D.; Schultz, A. J.; Hunter, B. A.; Wagner, J. L.; Chou, F. C.; Johnston, D. C. *Phys. Rev. B* **1993**, *48*, 499.
(32) Jorgensen, J. D.; Dabrowski, B.; Pei, S.; Hinks, D. G.; Soderholm, L.; Morosin, B.; Schirber, J. E.; Venturini, E. L.; Ginley, D. S. *Phys. Rev. B* **1988**, *38*, 11337.
(33) Chaillout, C.; Cheong, S. W.; Fisk, Z.; Lehmann, M. S.; Marezio, M.; Morosin, B.; Schirber, J. E. *Physica C* **1989**, *158*, 183.
(34) Chaillout, C.; Chenavas, J.; Cheong, S. W.; Fisk, Z.; Marezio, M.; Morosin, B.; Schirber, J. E. *Physica C* **1990**, *170*, 87.
(35) Locquet, J.-P.; Arrouy, F.; Machler, E.; Despont, M.; Bauer, P.; Williams, E. J. *Appl. Phys. Lett.* **1996**, *68*, 1999.
(36) Vaknin, D.; Zarestky, J. L.; Johnston, D. C.; Schirber, J. E.; Fisk, Z. *Phys. Rev. B* **1994**, *49*, 9057.
(37) Rial, C.; Moran, E.; Alario-Franco, M. A.; Amador, U.; Andersen, N. H. *Physica C* **1997**, *278*, 122.
(38) Lees, S. T.; Edwards, P. P.; Gameson, I.; Jones, M. O.; Slaski, M.; Rial, C.; Amador, U.; Moran, E. *Adv. Mater.* **1997**, *9*, 823.
(39) Xiong, X.; Zhu, Q.; Li, Z. G.; Moss, S. C.; Feng, H. H.; Hor, P. H.; Cox, D. E.; Bhavaraju, S.; Jacobson, A. J. *J. Mater. Res.* **1996**, *11*, 2121.
(40) Tranquada, J. M.; Kong, Y.; Lorenzo, J. E.; Buttrey, D. J.; D. E. Rice, E.; Sachan, V. *Phys. Rev. B* **1994**, *50*, 6340.

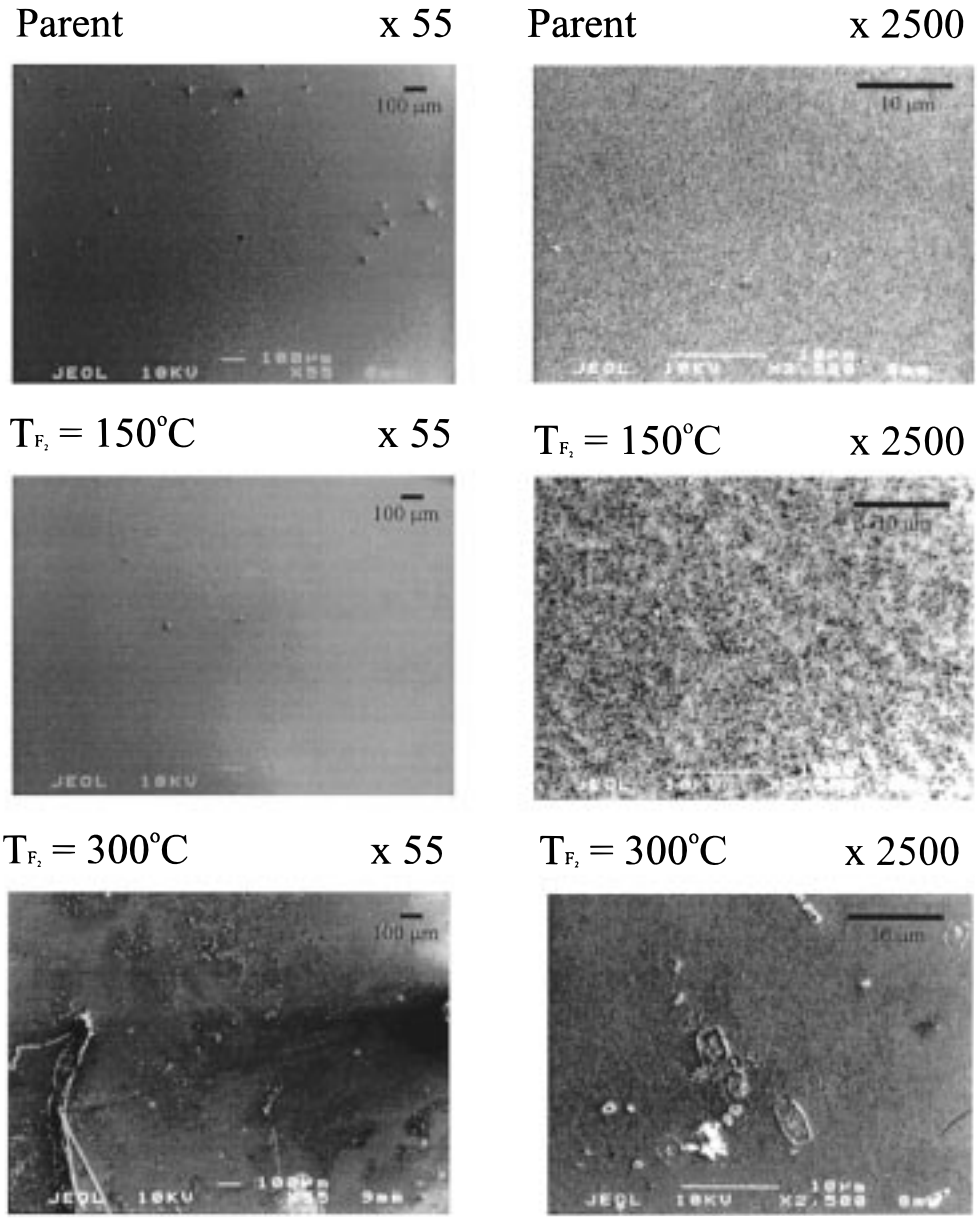

Figure 8. SEM micrographs of a parent La_2CuO_4 thin film and of La_2CuO_4 films fluorinated at T_{F_2} = 150 and 300 °C under magnifications of ×55 and ×2500.

From the micrographs of the three films taken at a magnification of ×55 it is clear that the parent La_2CuO_4 film is relatively smooth and homogeneous in appearance. The light spots that are scattered across its surface are commonly known as "boulders" and are the result of molten droplets being expelled from the target surface during the ablation process. The ×55 micrograph for the T_{F_2} = 150 °C film has a virtually identical appearance to that from the parent. Again, the film is relatively smooth, with just occasional boulders embedded in its surface, and there is no evidence of any damage caused by the fluorination. The T_{F_2} = 300 °C film, however, has a markedly different surface appearance under a magnification of ×55 than the parent film. The micrograph shows that its surface is very inhomogeneous in appearance, possessing numerous damaged and marked regions. There are a large number of light spots across the micrograph, but these do not have the same appearance as the boulders seen in the micrographs of the parent and T_{F_2} = 150 °C films. We believe that their origin is thus more likely to stem from the results of chemical fluorination rather than the ablation process.

The micrographs of the three films taken at higher magnification (×2500) reveal further detailed information concerning the effect of fluorination on surface morphology. Again, the micrograph of the parent film reveals its surface to be smooth and homogeneous in appearance, with the light spots corresponding to a low concentration of small boulders. The T_{F_2} = 150 °C film, however, has a different appearance to the parent film under this higher magnification. The micrograph exhibits considerable relief contrast, which implies that the 150 °C fluorination process has roughened its surface, causing partial pitting across the film. The higher magnification micrograph for the T_{F_2} = 300 °C film has a relief contrast that is dominated by the large damaged areas in the central region.

Magnetic Properties. To establish whether the fluorinated films were superconducting, magnetic mea-

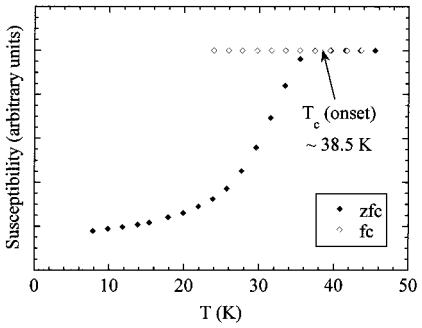

Figure 9. Magnetic susceptibility versus temperature trace for the La_2CuO_4 thin film fluorinated at $T_{F_2} = 150$ °C showing zero field cooled (zfc) and field cooled (fc) behavior.

surements were recorded using a SQUID magnetometer. A typical sequence involved measurement of the magnetization of the sample as a function of temperature after it had been first cooled in the absence of a magnetic field (zero field cooled—zfc) and then as it was cooling back down in the presence of the magnetic field used for the measurement (field cooled—fc). The applied magnetic field used for each measurement was 2×10^{-4} T. A parent La_2CuO_4 thin film was examined for superconducting properties in case ablation in the oxygen atmosphere had produced any superconducting $La_2CuO_{4+\delta}$.[12−14] The parent film did not exhibit superconductivity down to 5 K.

All of the films fluorinated in the range 70 °C ≤ T_{F_2} ≤ 250 °C exhibit superconducting properties, while the films fluorinated at $T_{F_2} = 40$ and 300 °C are nonsuperconducting. A magnetic susceptibility versus temperature plot for the $T_{F_2} = 150$ °C film is shown in Figure 9. The film superconducts with a T_c (onset) of 38.5 (±1) K, which compares favorably with that reported for the bulk material (up to 40 K).[22,23] The marked divergence in the zfc and fc data below T_c can be attributed to type-II superconductor flux pinning effects. The zfc data show a single smooth transition to the superconducting state and this is typical of all the superconducting fluorinated films. Despite the X-ray data indicating the presence of two phases in the majority of the films, there is no evidence of two superconducting transitions in any of the susceptibility plots. This implies that only one of the constituent phases in each film is superconducting or that both phases have virtually identical transition temperatures. Equally, it could be that the diamagnetic signal from one phase is extremely strong and thus masks the signal from the other phase.

In Figure 10 we show the dependence of T_c (onset) on T_{F_2} for the range of fluorinated La_2CuO_4 thin films. The plot reveals how T_c (onset) rises from 0 K for films fluorinated at T_{F_2} < ca. 40 °C to a maximum of ca. 38.5 K for films fluorinated at 140−150 °C before gradually falling back to 0 K for films fluorinated at T_{F_2} > ca. 270 °C. Hence, in terms of T_c, the optimum fluorination conditions for La_2CuO_4 thin films correspond to a static anneal under 10% F_2 in N_2 for 10 min at a temperature of 140−150 °C. Once again, it is interesting to make comparisons between our results on thin films and the results quoted for fluorinated, bulk samples of La_2CuO_4. The optimum fluorination conditions for the bulk material correspond to an anneal under 1.3 bar of pure F_2 gas for 20 h at a temperature of 200 °C.[22,23] This comparison not only highlights the extreme reactivity

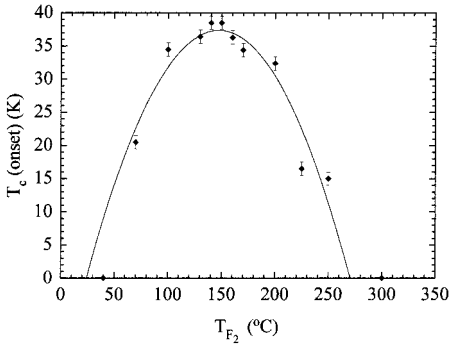

Figure 10. Variation of T_c (onset) with the fluorination temperature, T_{F_2}, for fluorinated La_2CuO_4 thin films.

of thin film materials but also demonstrates the relative ease with which successful thin film fluorination can be achieved under optimized conditions.

The form of the data presented in Figure 10 is reminiscent of many high T_c systems where the degree of hole doping can be continuously varied (cf. the schematic representation shown earlier in Figure 2). Our interpretation of this is that at low fluorination temperatures, i.e., T_{F_2} < 140 °C, the material is underdoped with fluorine; at $T_{F_2} = 140-150$ °C it is optimally doped, and for T_{F_2} > 150 °C it is overdoped. Furthermore, if this proposition is correct, one would expect a change in the lattice constants of the superconducting phase with T_{F_2}. As can be seen in Table 2, of the two expanded phases, the *c*-lattice parameter of the larger of these phases increases with T_{F_2}, while the *c*-lattice parameter of the smaller phase remains constant. The available X-ray data (which, of course, only yield information concerning the *c*-lattice parameters) therefore suggest that the superconducting phase is that with the larger *c* parameter.

Further support for this proposition can be obtained by examining the X-ray data recorded on the nonsuperconducting $T_{F_2} = 40$ °C film. Table 2 shows that this film consists of a mixture of the parent La_2CuO_4 material and a fluorinated La_2CuO_4 phase with a *c*-lattice parameter of 13.218 Å. As this film is nonsuperconducting, it follows that the extent of fluorine-doping that causes an increase in the *c*-lattice parameter to 13.218 Å provides an insufficient number of hole carriers to induce superconductivity within the film. The smaller stable phase with a *c*-lattice parameter of ca. 13.20 Å, which is present in all of the films fluorinated in the range 100 °C ≤ T_{F_2} ≤ 170 °C, is therefore unlikely to have sufficient carriers to exhibit superconducting properties.

It is also likely that the reduction in crystallinity of these films for T_{F_2} > 200 °C plays a significant contributory role to the observed fall in their T_c (onset). Conversely, the X-ray data recorded on the films fluorinated at T_{F_2} ≤ 170 °C reveal that these films have preserved their high crystallinity and so it is likely that the degree of fluorine doping will be more significant than crystallinity effects in governing their values of T_c-(onset). Figure 10 shows that our parabola has passed through its maximum value of T_c(onset) before reduction in film crystallinity becomes significant and we therefore believe that our optimal fluorination conditions are derived purely from doping levels within the films. These magnetic results demonstrate that our fluorina-

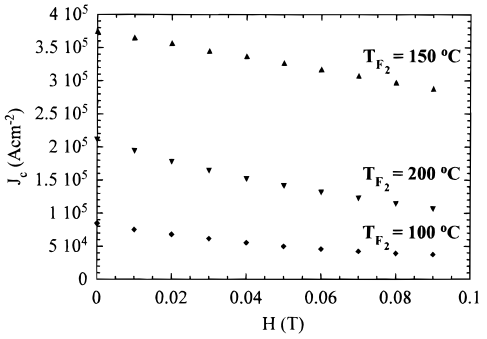

Figure 11. Critical current density, J_c (calculated from SQUID data), versus applied magnetic field at 10 K for La_2CuO_4 thin films fluorinated at $T_{F_2} = 100$, 150, and 200 °C.

tion technique is of sufficient sensitivity to provide a controlled method for the continuous hole-doping of thin film materials.

The S100 SQUID magnetometer was also employed to record magnetization versus applied magnetic field hysteresis loops on La_2CuO_4 thin films that were fluorinated in the range 100 °C $\leq T_{F_2} \leq$ 200 °C. The loops enable calculation of the critical current densities, J_c. The films were mounted with their surfaces directed perpendicular to the applied magnetic field so that critical currents flowed entirely in the *ab* plane. All measurements were taken at 10 K over the applied magnetic field range of 0.0−0.1 T. The J_c values are deduced from the hysteresis loops by assuming the so-called Bean model with a uniform J_c within the *ab* plane of the film and uniform penetration of flux from the edges.[41,42]

The calculated J_cs at 10 K for the La_2CuO_4 thin films fluorinated at 100, 150, and 200 °C are plotted as a function of applied magnetic field, *H*, in Figure 11. The $T_{F_2} = 150$ °C film has the largest J_c values across the applied magnetic field range. Indeed, the trace from the $T_{F_2} = 150$ °C film shows that in the absence of an applied field, the film can carry a current density of up to ca. 3.8×10^5 A cm^{-2}. This is a respectable value, but other superconducting copper oxide systems have superior J_c characteristics (e.g., optimally grown thin films of $YBa_2Cu_3O_{7-\delta}$ possess zero field J_c values of ca. 5×10^6 A cm^{-2} at a temperature of 77 K[43]).

In Figure 12 we show the dependence of J_c in zero field on T_{F_2} of the La_2CuO_4 thin film at 10 K. Although the data appear somewhat irregular, the general trends show first an increase in J_c as T_{F_2} is raised from 100 to 150 °C (from $\sim 0.8 \times 10^5$ to $\sim 3.8 \times 10^5$ A cm^{-2}) and then a decrease as the fluorination temperature is raised further (down to $\sim 2.0 \times 10^5$ A cm^{-2} for $T_{F_2} = 200$ °C). Interestingly, this mirrors the trends observed with the dependence of T_c on T_{F_2}, implying that the optimal fluorination temperature for La_2CuO_4 thin films is 150 °C, in terms of both T_c and J_c.

Having established that the $T_{F_2} = 150$ °C thin film has the largest J_c values, a 12 T vibrating sample magnetometer (VSM) was employed to record magnetization versus applied magnetic field loops on this film

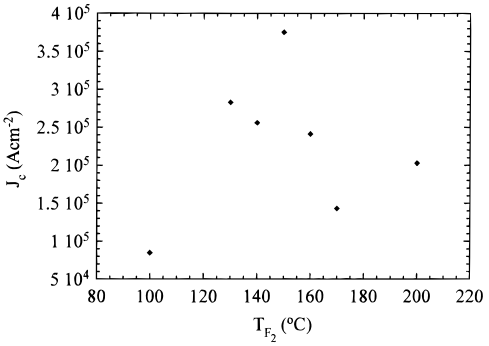

Figure 12. Critical current density, J_c (calculated from SQUID data), versus fluorination temperature, T_{F_2}, for fluorinated La_2CuO_4 thin films at 10 K in zero applied magnetic field.

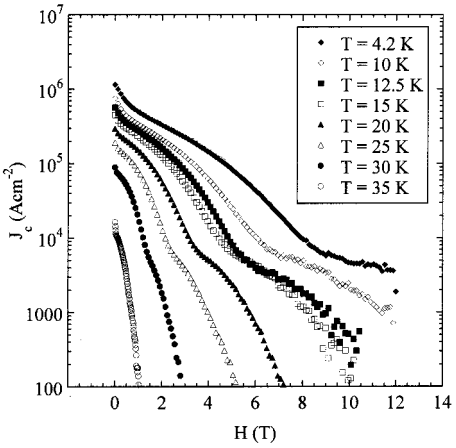

Figure 13. Applied magnetic field dependence of J_c (calculated from VSM data) at several temperatures for the La_2CuO_4 thin film fluorinated at $T_{F_2} = 150$ °C.

over much larger field ranges than is possible with the SQUID. The hysteresis loops were measured over a range of different temperatures below T_c with the applied magnetic field again directed perpendicular to the surface of the film. J_c values have been calculated from these VSM data in exactly the same way as from the SQUID data, by application of the Bean model.[41,42]

The results of these calculations are shown in Figure 13, which presents the applied magnetic field dependence of J_c at several temperatures for the La_2CuO_4 thin film fluorinated at $T_{F_2} = 150$ °C. The deterioration of J_c as the applied field is increased from 0 to 3 T is relatively slow for measurements taken in the range 4.2−15 K. However, as the temperature is raised, J_c falls increasingly rapidly with increasing applied field. This is best exemplified by comparing the data respectively recorded at 4.2 and 35 K. At 4.2 K, J_c falls by approximately half an order of magnitude as the field is increased from 0 to 1 T. At 35 K, however, over the same field range, J_c is reduced by approximately 2 orders of magnitude. Figure 13 also shows that each J_c trace decays in an inhomogeneous fashion, passing through different regimes as the applied magnetic field is varied. These different regimes are probably caused by conflicting and competitive flux pinning mechanisms within the film.

Close inspection of Figure 13 shows that at 10 K and in the absence of an applied magnetic field, the $T_{F_2} = 150$ °C film has a J_c of ca. 7.6×10^5 A cm^{-2}. As shown

(41) Bean, C. P. *Rev. Mod. Phys.* **1964**, *36*, 31.
(42) Gyorgy, E. M.; van Dover: R. B.; K. Jackson, A.; Schneemeyer, L. F.; Waszczak J. V. *Appl. Phys. Lett.* **1989**, *55*, 283.
(43) Qiu, X. G.; Cui, C. G.; Zhang, Y. Z.; Li, S. L.; Zhao, Y. Y.; P. Xu, P.; Li, L. *J. Appl. Phys.* **1990**, *68*, 884.

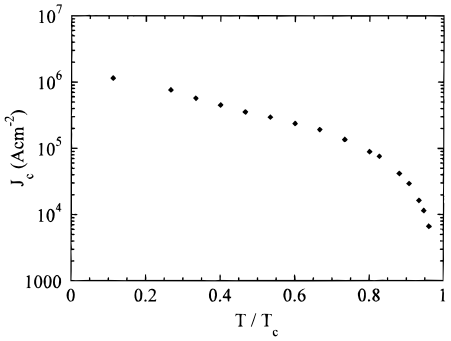

Figure 14. Reduced temperature dependence of J_c (calculated from VSM data) for the La_2CuO_4 thin film fluorinated at T_{F_2} = 150 °C in zero applied magnetic field.

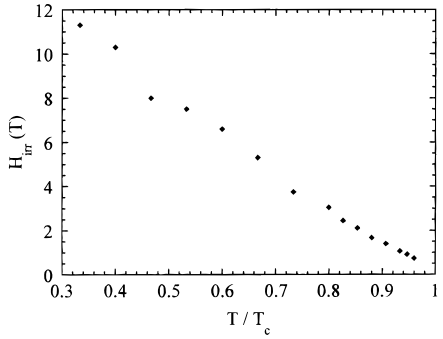

Figure 15. Irreversibility line for the La_2CuO_4 thin film fluorinated at T_{F_2} = 150 °C using 5×10^{-9} A m^2 as the criterion for irreversible behavior.

earlier, the SQUID data yield a value for J_c of ca. 3.8×10^5 A cm^{-2} under identical conditions on the same film. The reason for the VSM data yielding J_c values which are a factor of 2 larger than those from the SQUID stems from the way measurements are taken on these two pieces of apparatus. In the SQUID magnetometer, measurements are recorded after the applied field has oscillated about its required value. Data points are thus only taken when the sample has completely equilibrated with the applied field. In the VSM, however, measurements are recorded while the applied magnetic field is continually ramping (in this work the ramp rate was 15 mT s^{-1}). Data points are thus taken when the sample may not have completely equilibrated with the applied field. This accounts for the observed differences in J_c values and indicates that the results from the SQUID data are likely to be more accurate than those from the VSM data.

Figure 14 presents the temperature dependence of the VSM calculated J_c in the absence of an applied magnetic field for the T_{F_2} = 150 °C La_2CuO_4 thin film. At low temperatures, J_c reaches a maximum of over 10^6 A cm^{-2}, a value which is quite respectable for thin film superconducting materials. The deterioration in J_c with increasing temperature is relatively slow over the majority of the temperature range, i.e., between 0 and 0.8 on the reduced temperature scale J_c falls by approximately 1 order of magnitude. The final rapid decrease in J_c with increasing temperature indicates that the superconductivity of the film is a bulk property.

The irreversibility line, which plots the value of the applied magnetic field (H_{irr}) required to destroy the irreversible behavior for the film at different temperatures, is shown in Figure 15. Each data point has been calculated from the VSM magnetization versus applied field hysteresis loops using 5×10^{-9} A m^2 as the criterion for irreversible behavior. The graph shows that at low temperatures, applied fields of over 12 T are required to completely suppress high-temperature superconductivity in the fluorinated cuprate films.

Conclusions

Superconducting properties have been successfully induced in pulsed laser-ablated, semiconducting thin films of La_2CuO_4 by a postdeposition, ex-situ gas-phase fluorination approach. Our method therefore allows the facile anionic modification of the carrier concentration within deposited thin film materials.

Variation of T_{F_2} has revealed that the fluorination proceeds in three separate stages. For T_{F_2} < 100 °C, the fluorinated films consist of the parent phase and a *c*-axis expanded phase. For 100 °C ≤ T_{F_2} < 200 °C, the parent phase has been eliminated and the films consist of two *c*-axis expanded phases, implying that there is a disproportionation of fluorine uptake. The smaller of these phases has a relatively constant *c*-lattice parameter (ca. 13.20 Å) and is believed to be nonsuperconducting, while the larger phase has a *c*-lattice parameter that does exhibit a dependence on T_{F_2}, and it is this phase that is thought to be responsible for the superconducting properties within the films. For T_{F_2} ≥ 200 °C, the fluorination causes a significant reduction in the crystallinity of the films and eventually a partial decomposition into LaF_3 and CuF_2. These structural properties differ markedly from those observed on bulk fluorinated samples of La_2CuO_4; as far as we are aware, there are no reports of any disproportionate or phase segregation following the uptake of fluorine within such samples.

The La_2CuO_4 thin film fluorinated at T_{F_2} = 150 °C has the largest T_c and J_c values. The T_c of 38.5 (±1) K compares favorably with results from bulk samples and the VSM calculated J_c of >10^6 A cm^{-2} in zero field at 4.2 K is respectable for a superconducting thin film material. The irreversibility line of the film has been established, revealing that at low temperatures, applied magnetic fields of in excess of 12 T are required to completely destroy the superconductivity.

This postdeposition, ex-situ fluorination methodology appears to be of sufficient sensitivity to allow a degree of control to the level of hole-doping within the La_2CuO_4 thin films (Figure 10); this extent of control has not previously been observed with gas-phase fluorination procedures. Having established the feasibility of this method to manipulate the carrier concentration in thin films of La_2CuO_4, we are currently extending our study to assess its potential in other high T_c systems.

Acknowledgment. We thank Dr. Philip Woodall and Dr. Fee Wellhofer (laser-ablation), Dr. Ian Langford and Ron Pflaumer (X-ray diffraction), Sue Dipple (SEM), and David Norris (RBS) for their considerable assistance in this project. We also thank the EPSRC and GEC-Marconi Ltd. (CASE studentship to S.T.L.) for financial support. P.P.E. thanks the Royal Society for the award of a Leverhulme Senior Research Fellowship.

CM9802752